Hardening and crystallization in monatomic metallic glass during elastic cycling

Ronggen Cao
Department of Materials Science, Fudan University, Shanghai 200433, China

Yun Deng
Key Laboratory of Magnetic Resonance in Biological Systems, Wuhan Institute of Physics and Mathematics, Chinese Academy of Sciences, Wuhan 430071, China

Chuang Deng[a)]
Department of Mechanical Engineering, The University of Manitoba, Winnipeg, Manitoba R3T 5V6, Canada

(Received 16 January 2015; accepted 22 April 2015)

While conventional metallic glass (MG) is usually an alloy that contains at least two types of different elements, monatomic metallic glass (MMG) in body-centered cubic metals has recently been vitrified experimentally through ultrafast quenching. In this research, MMG in Ta was vitrified by molecular dynamics simulations and used as a model system to explore the atomistic mechanism of hardening in MG under cyclic loading well below the yield point. It was found that significant structural ordering was caused during the elastic cycling without accumulating apparent plastic strain, which ultimately led to the crystallization of MG that has been long conjectured but rarely directly proved before. It was also revealed that tensile stresses were more likely to induce structural ordering and crystallization in MG than compressive stresses.

I. INTRODUCTION

The mechanical properties of materials are strongly linked with their microstructural evolution under external loading. Whereas structural defects such as dislocations have been found to govern the microstructural evolution and mechanical properties in crystalline materials, no such defects have been unambiguously identified in amorphous materials such as metallic glass (MG). Therefore, despite the significant efforts that have been made in the past,[1–13] the microstructural evolution that leads to various mechanical responses in MGs is still under debate, among which the cyclic hardening within the elastic regime[8–13] has drawn considerable attention in recent years. It has been widely reported that the yield strength of MGs can be significantly increased by cycling the sample with small amplitude, which can significantly impact the fracture and fatigue behavior of the MGs.[8–13]

Although no apparent plastic strain or macroscopic shear banding can be detected during the elastic cycling in MG, it has been conjectured that substantial microstructural ordering or even nanocrystallization has occurred.[8–10] Recently, Wang et al.[11] found that nanocrystals can be formed at a semicircle notch-tip region in cyclically strained MG based on in situ TEM experiments. However, the molecular dynamics (MD) simulations performed by Wang et al.[11] also suggested that before the formation of the nanocrystal, the region around the notch-tip has experienced severe plastic deformation due to the strong stress concentration at the notch-tip even though the overall cycling strain was below the yield point. To date, no direct experimental evidence has been reported to confirm the formation of nanocrystals in MG due to purely elastic cycling.

On the other hand, atomistic simulations which tried to find nanocrystals in a CuZr MG during elastic cycling under nanoindentation[8] also proved unfruitful. It may be because the crystallization process in CuZr-based MG is too slow to be observed in typical MD simulations. In principle, such limitations can be overcome by choosing a MG that crystallizes fast enough to be observed in the MD timescale (~ns). While conventional multicomponent MGs do not usually satisfy this criteria, Zhong et al.[14] reported the formation of monatomic MGs (MMGs) in Ta and V through ultrafast liquid quenching in a recent research, which opened the door for a new category of MGs. Since monatomic metals tend to form crystalline structure to minimize the energy, MMGs should crystallize more easily as compared to multicomponent MGs, which may be detectable within the MD timescale.

The purpose of this research is to vitrify MMGs by MD simulations, and use them as model systems to explore the hardening and crystallization in MG due to elastic cycling. The influences of key parameters such as

Contributing Editor: Franz Faupel
[a)]Address all correspondence to this author.
e-mail: dengc@ad.umanitoba.ca
DOI: 10.1557/jmr.2015.130

 © Materials Research Society 2015

https://doi.org/10.1557/jmr.2015.130 Published online by Cambridge University Press

the system temperature, the cycling amplitude, and the boundary conditions on the structural ordering and crystallization in MMGs will be systematically analyzed and discussed.

II. SIMULATION METHODS

To be consistent with the experimental work by Zhong et al.,[14] Ta was selected as a model system in this research. Specifically, the vitrification of Ta was simulated through ultrafast liquid quenching by using MD with the LAMMPS[15] package. The timestep was 5 fs, which was selected to be more efficient while still producing results as accurate as when a timestep of 1 fs was used. The interatomic forces were characterized by embedded-atom potential for Ta.[16] At the beginning of the simulation, a block of single crystalline Ta (~33.0 nm × 6.6 nm × 13.2 nm) with periodic boundary in x, y, and z directions [Fig. 1(a)] was first constructed and liquefied by heating to a target temperature of T_{Ta} = 4200 K within 100 ps. The sample was equilibrated at the liquid state for 100 ps and quenched to 300 K at the rates between 1.56 and 39 K/ps. As a reference, the quenching rate used by Zhong et al.[14] to vitrify Ta in their experiments was between 50 and 100 K/ps. All simulations were performed under zero pressure by using isobaric–isothermal ensemble (NPT). The atomic configurations were visualized by using AtomEye.[17]

III. RESULTS

A. Vitrification of Ta

The atomistic configurations and the radial distribution function (RDF) of the quenched Ta were examined and compared to that in the crystalline and liquid phase, respectively, which showed that the as-quenched samples were amorphous when the cooling rate was high. Specifically, crystallization was observed in Ta at the cooling rate of 1.56 K/ps. Figure 1(a) shows the atomistic configuration of a representative Ta MG after being quenched to 300 K. Furthermore, the RDF of two Ta samples quenched at 1.95 K/ps (Ta-quenched-01) and 39 K/ps (Ta-quenched-02), respectively, was computed and compared to crystalline Ta [Fig. 1(b)], which shows clear amorphous characteristics of the two as-quenched Ta samples. To validate if the as-quenched samples would behave the same as typical multicomponent MGs, the evolution of the atomic volume during the cooling in both samples is plotted in Fig. 1(c). For comparison, the evolution of the atomic volume of the Ta-quenched-01 sample during the reheating to T = 4200 K at two different rates of 7.8 K/ps (Ta-reheated-01) and 1.95 K/ps (Ta-reheated-02) is also included in Fig. 1(c).

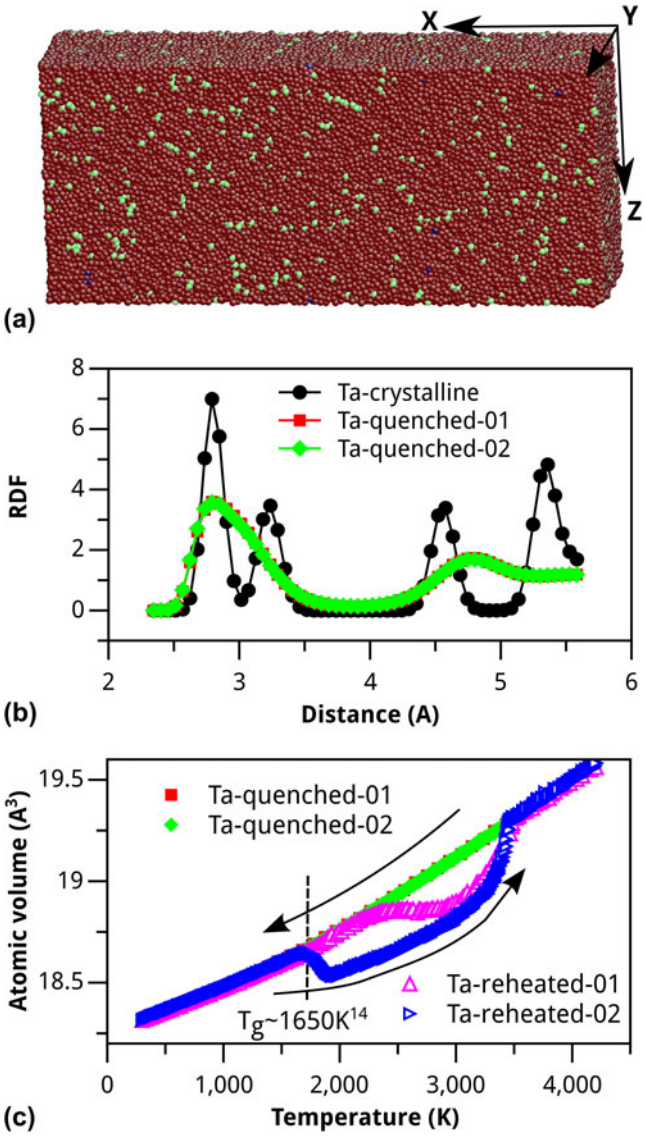


FIG. 1. (a) Atomistic configuration of the as-quenched Ta sample at 300 K. (b) RDF of the crystalline and as-quenched Ta samples at 300 K. (c) Evolution of the atomic volume of Ta during the quenching and reheating at different rates. The atoms in (a) were colored according to CNA.

It was found that the two cooling curves overlapped each other in Fig. 1(c) and both showed glass transition at T_g ~ 1700 K as marked by the vertical dashed line, which was estimated by a slope change at this temperature. For comparison, the glass transition temperature in Ta has been determined to be T_g ~ 1650 K by Zhong et al. in their experiments.[14] In contrast, the two reheating curves showed dramatically different crystallization temperatures and neither of them overlapped the two cooling curves. While the glass transition at T ~ 1700 K is a clear sign of the formation of MG, the asymmetric heating and cooling behavior have also been widely recognized as one key characteristic of conventional multicomponent MGs.[18–20]

https://doi.org/10.1557/jmr.2015.130 Published online by Cambridge University Press

B. Hardening in MMG Ta due to elastic cycling

Since Ta was found to vitrify and crystallize within reasonable MD timescale, the MMG Ta (Ta-quenched-01) was used for all subsequent elastic cycling. In the following, all simulations were performed at $T = 1000$ K. According to Fig. 1(c), the relatively high temperature ($T = 1000$ K) would aid the microstructural evolution in Ta MMG during external loading without causing glass transition or crystallization by thermal effects alone. For example, the sample has been tested by performing purely thermal equilibration at $T = 1000$ for up to 10 ns and no crystallization or other substantial structural change has been observed. As shown in Fig. 2(a), free boundary conditions were applied to MMG Ta (Ta-quenched-01) on the two surfaces perpendicular to x-direction during the elastic cycling (e.g., periodically tensile and compressive loading) along z-direction [the x-, y-, and z-directions are defined in Fig. 1(a)]. The deformation was applied at a constant rate of $\sim \pm 5 \times 10^8$/s, which is typical for MD simulations. The cycling amplitude was relatively small ($\varepsilon \pm 1.25\%$) to ensure that the loading was in the elastic regime. Figures 2(b) and 2(c) show the stress evolution during the loading as a function of time and strain, respectively. It can be seen in both figures that the cycling was elastic and there was no accumulation of plastic strain during the cycling. The Ta MMG samples with different numbers of elastic cycles were then loaded under monotonic tensile deformation; the corresponding stress–strain curves are shown in Fig. 2(d). The inset of Fig. 2(d) clearly indicates that the maximum tensile strength increased with the increasing number of elastic cycles, which is consistent with previous reports on cyclic hardening in MG under nanoindentation.[9,10] Furthermore, a saturation of the hardening effect that has been reported before[8–10] is also indicated in Fig. 2(e). It can be seen that the increase in average flow stress between 4.25 and 5.5% tensile strain (or the hardening effect) became less pronounced and eventually saturated as the number of elastic cycles increased.

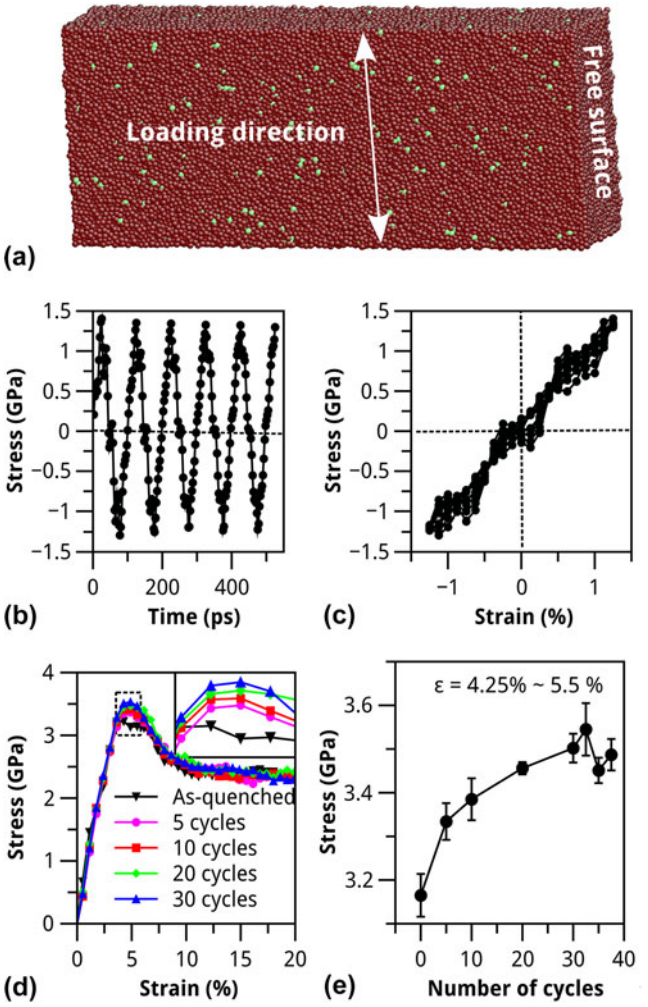


FIG. 2. (a) Atomistic configuration of the Ta MMG with free surfaces in the x-direction under cyclic loading. (b) The stress versus time during the cyclic loading. (c) The stress versus strain during the cyclic loading. (d) The stress–strain curves of the pre-cycled Ta MMG samples during monotonic tensile loading. The inset indicates the change of the maximum tensile strength due to the elastic cycling. (e) The average tensile stress between 4.25 and 5.5% tensile strain as a function of the number of elastic cycles. The atoms in (a) were colored according to CNA.

C. Crystallization in MMG Ta during elastic cycling

To explore the atomistic mechanisms that led to the hardening in MMG Ta during the elastic cycling, we performed more simulations in different Ta samples and carefully examined the microstructural evolution during the elastic cycling by common neighbor analysis (CNA). As shown in Fig. 3(a), a crack (~2 nm × 7 nm × 1 nm) was introduced to the free surface of the Ta MMG (Ta-SPP-crack) so that the results could be compared with that from Wang et al.[11] The influences of free surfaces were also evaluated by simulating a Ta MMG sample with periodic boundary conditions in x, y, and z directions [Fig. 3(e), Ta-PPP]. The cycling amplitude was $\varepsilon = \pm 2.5\%$ in the Ta-PPP sample and $\varepsilon = \pm 1.25\%$ in the Ta-SPP-crack and Ta-SPP samples. It can be seen from the insets of Fig. 3 that in all the three Ta MMG samples the peak stress increased dramatically when a certain number of elastic cycles was reached, which corresponded to the formation of nanocrystals. Representative snapshots are shown in Figs. 3(b), 3(d), and 3(f) for the samples of Ta-SPP-crack, Ta-SPP, and Ta-PPP, respectively, after $n = 22$, 35, and 33 rounds of cycling. In each sample, the nanocrystal (the region with blue atoms) was identified to have a body-centered cubic structure based on CNA. It is important to note that the number of elastic cycles that were needed to cause the saturation of hardening effects as observed in Fig. 2 (e.g., when the number of

https://doi.org/10.1557/jmr.2015.130 Published online by Cambridge University Press

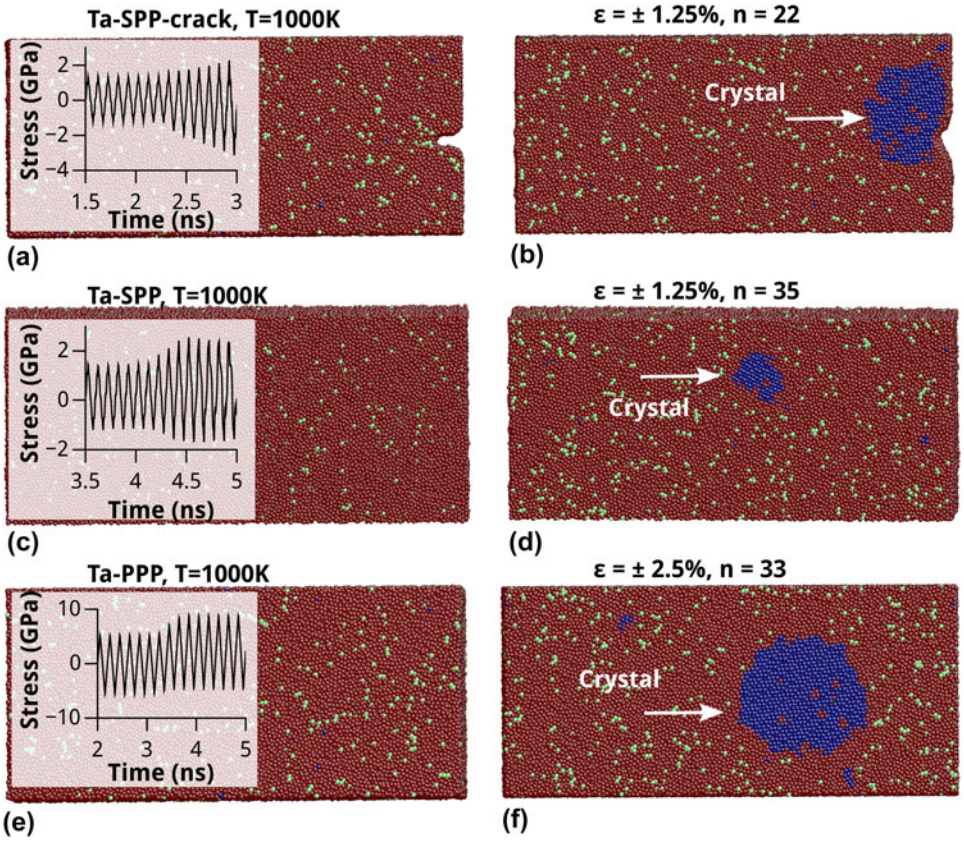


FIG. 3. The atomistic configuration of Ta MMG samples with (a) free boundaries and a crack, (c) free boundaries, and (e) periodic boundaries in *x*-direction. The inset in (a), (c), and (e) shows the corresponding stress evolution during the cycling in each Ta MMG sample. (b), (d), and (f) show the formation of a nanocrystal due to the cycling in each Ta MMG sample, as indicated by the arrow. The atoms were colored according to CNA.

elastic cycles reached $n > 30$) were consistent with that required to initiate crystallization. Therefore, it is now possible to explain the hardening effects observed in Fig. 2 by gradual structural relaxation during elastic cycling, which could eventually lead to dramatic ordering and crystallization in MMG Ta samples.

It is worth mentioning that in the Ta-SPP-crack sample, fewer cycles were needed to form a nanocrystal as compared to the sample with no crack (Ta-SPP). Moreover, the nanocrystal was formed at the crack region in the Ta-SPP-crack sample but near the center in the Ta-SPP sample. This observation was consistent with Wang et al.[11] that the crack can serve as stress concentration to facilitate the nucleation of nanocrystal during cyclic loading. More importantly, Fig. 3(f) proves the conjecture that cyclic loading within the elastic regime (e.g., at strains well below the yield point) can cause significant ordering and ultimately lead to the formation of nanocrystals in MGs even when stress concentrators such as cracks or free surfaces are absent. In contrast, no substantial structural change was found in the Ta-SPP sample during monotonic loading up to 20% tensile strain [Fig. 2(d)].

IV. DISCUSSION

A. Influences of loading mode

Since the Ta MMG samples experienced both tension and compression during the elastic cycling, it is interesting to find out which loading mode was more effective in inducing the structural ordering and crystallization in them. For this purpose, the average energy per atom in the Ta-SPP sample was plotted versus time during the elastic cycling, as shown in Fig. 4. Two cycling amplitudes, $\varepsilon = \pm 1.25\%$ and $\varepsilon = \pm 2.5\%$, were considered. The results in the sample with no cycling ($\varepsilon = \pm 0\%$) were also included. It was found in Fig. 4 that there was an overall trend of decrease in the average energy per atom even when no cycling was applied. This trend was expected since MG in general is far away from its equilibrium state and the Ta-SPP sample was initially stuck at a relatively high energy state due to the rapid quenching. Nevertheless, the rate of energy decrease gradually dropped as a function of the relaxation time and the thermal effects alone ($T = 1000$ K) could not relax the Ta MMG into the crystalline phase within reasonable MD simulation time. In contrast, although the

https://doi.org/10.1557/jmr.2015.130 Published online by Cambridge University Press

average energy per atom dropped and rose during the cycling, there was a general trend of energy decrease during the elastic cycling and the rate of energy decrease became steeper with the increased number of cycling. The onset of crystallization can be clearly identified in Fig. 4 by the sudden drop of energy, e.g., $t \approx 4.2$ and 1.2 ns for the Ta MMG with a cycling amplitude of $\varepsilon = \pm 1.25\%$ and $\varepsilon = \pm 2.5\%$, respectively. What is more, it can be seen in the inset of Fig. 4 that the tension and compression caused dramatically asymmetric effects on the structural relaxation of the Ta MMG. Specifically, the half cycles during tension caused significantly higher energy rise in the Ta MMG than during compression. In particular, the energy variation during the compression in Ta MMG with a cycling amplitude of $\varepsilon = \pm 1.25\%$ was hardly sensible. It can thus be concluded that the structural ordering and crystallization in Ta MMG during the elastic cycling [e.g., Fig. 3(d)] were mainly caused by the tensile loading. In other words, the Ta MMG can be activated more effectively to overcome the energy barrier for crystallization under tension than under compression.

B. Influences of temperature

Although it has been found that at $T = 1000$ K, the thermal effects alone could not cause the phase transformation from amorphous to crystalline in MMG Ta within reasonable MD time, it is believed that the high temperature should have at least facilitated the transformation during the elastic cycling. To separate the influences from stress and thermal effects on the crystallization in MMG Ta, it is important to investigate if crystallization can be caused by elastic cycling alone, for example, at lower temperatures. For this purpose, the elastic cycling was applied to MMG Ta (Ta-SPP and Ta-SPP-crack) at $T = 300$ and 50 K with a cycling amplitude of $\varepsilon = \pm 5\%$. To expedite the simulation, the deformation was applied at the strain rate of $\sim \pm 1 \times 10^9$/s at 300 K and $\sim \pm 5 \times 10^9$/s at 50 K, respectively. The cycling was elastic with one representative example shown in Figs. 5(a) and 5(b). It can be seen that the loading was symmetric during tension and compression with no accumulation of plastic strain during the cycling.

Crystallization was observed in both Ta-SPP and Ta-SPP-crack samples at $T = 300$ K while crystallization was only observed in the Ta-SPP-crack sample at $T = 50$ K within the simulation time of 10 ns. As shown in Fig. 5(c), crystals formed at two regions in the Ta-SPP sample at $T = 300$ K after $n = 62$ elastic cycles as indicated by the white arrows. It is important to note that one crystal was formed in the middle of the Ta-SPP sample which indicates that free surface was not a necessity for the crystallization in MMG Ta during the elastic cycling. In contrast, the crystal formed near the crack on the free surface in the Ta-SPP-crack sample at $T = 50$ K after $n = 269$ elastic cycles. It is

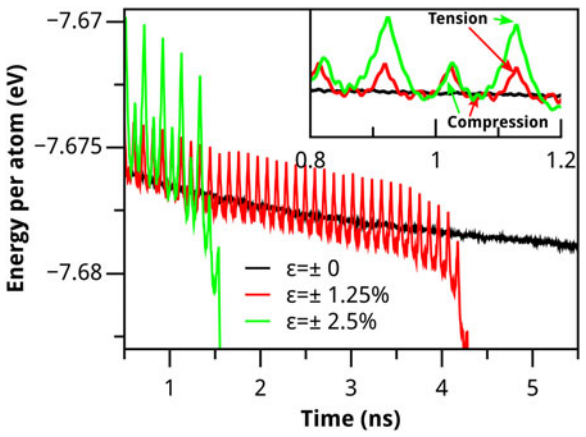


FIG. 4. The evolution of the average atomic energy in Ta MMG samples with different cycling amplitudes. The inset shows the zoomed view between 0.8 and 1.2 ns.

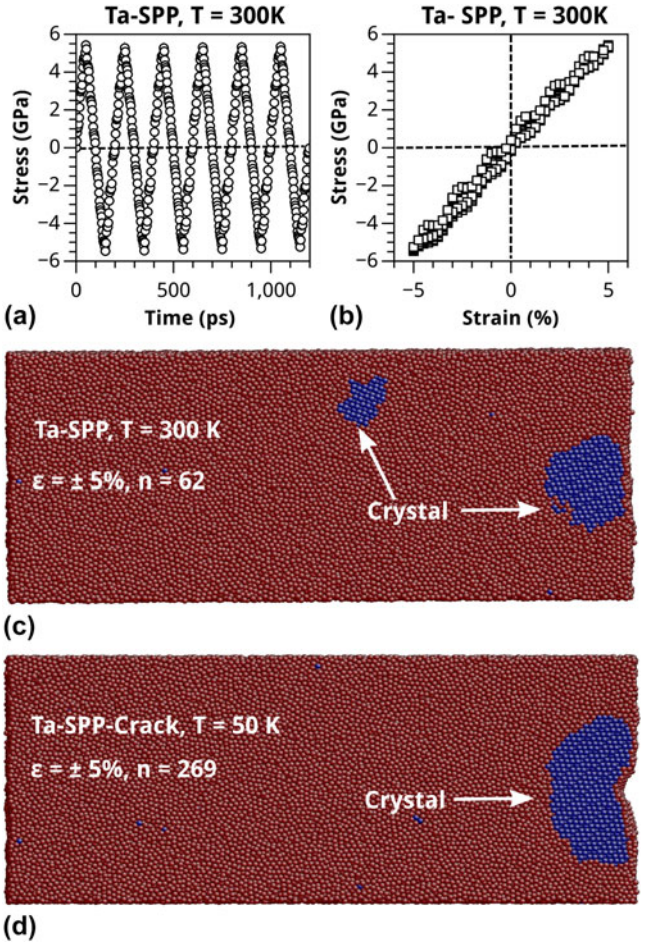


FIG. 5. The stress versus (a) time and (b) strain during the elastic cycling of the Ta-SPP sample at $T = 300$ K. The atomistic configuration showing the formation of nanocrystals in (c) Ta-SPP sample at $T = 300$ K and (d) Ta-SPP-crack sample at $T = 50$ K during the elastic cycling. The atoms in (c) and (d) were colored by CNA.

https://doi.org/10.1557/jmr.2015.130 Published online by Cambridge University Press

therefore confirmed that stress alone could induce the crystallization in MMG Ta.

C. Ultrafast liquid quenching of Cu

In the experimental work by Zhong et al.,[14] it has been reported that face-centered cubic metals cannot be vitrified by the same ultrafast liquid quenching method. To confirm if the atomistic simulation used in this work was consistent with the experimental method by Zhong et al.,[14] Cu was also simulated as a model system in face-centered cubic metals to see if MMG Cu can be vitrified in a similar way. Specifically, a block of single crystalline Cu (~36.4 nm × 7.3 nm × 14.6 nm) with periodic boundary in x, y, and z directions was constructed and simulated with the embedded-atom method potential of Cu.[21] The sample was then heated to liquid at T_{Cu} = 2000 K and quenched at different rates from 0.68 to 17 K/ps. It was found that partial crystallization occurred even at the highest quenching rate of 17 K/ps, e.g., a few tiny crystals were formed and embedded in the otherwise amorphous matrix. As shown in Fig. 6(a), the RDF of Cu gradually evolved during the quenching. While the RDF at relatively high temperatures of T = 850 and 1000 K was similar to that at the liquid state, the RDF at T = 300 K showed dramatically different features (e.g., splitted peaks at the atomic distance between 4 and 5.5 Å) which indicated a structural transition. In contrast, the Ta sample quenched at the rate of 1.95 K/ps (about 10 times slower than that in Cu) showed no apparent pattern change in the RDF [Fig. 6(b)], which suggested that the quenched Ta at T = 300 K maintained a similar structure to that in the liquid state.

The almost instantaneous crystallization in liquid Cu was further investigated by analysing the atomic volume evolution during the liquid quenching at different rates. As shown in Fig. 7, all curves overlapped each other when the temperature was higher than T = 1000 K. However, a change in slope around T = 800 K was found in all curves which suggested a structural transition at this temperature. The zoomed view further confirmed that the change was more significant at lower quenching rates, at which a larger degree of crystallization was observed. For example, while the two samples quenched at the rates of 0.85 and 0.56 K/ps were completely crystallized, small crystals were nucleated in the sample quenched at 1.7 K/ps as shown in the circled region of Fig. 7. It is worth mentioning that no difference can be found in the RDF of the samples quenched at rates between 17 and 1.13 K/ps. The results in Figs. 6 and 7 thus confirmed that face-centered cubic metals (e.g., Cu) are indeed more difficult to be vitrified than body-centered cubic metals with high melting points (e.g., Ta).

In this research, all simulations were limited to elastic cycling through uniaxial loading only. However, the unique properties of MMG Ta should make it particularly suitable for investigating the subtle microstructural evolution in general MGs under other circumstances by atomistic simulations. For example, since the MMGs were found to be highly sensitive to temperatures and external loading, some subtle microstructural evolutions such as the activation and coalescence of shear transformation zones[5–7,22] that are typical in general multicomponent MGs may be magnified and become easier to be identified and characterized in MMGs. On the other hand, since the microstructural evolution in MMGs is faster than that in conventional multicomponent MGs, some processes that are typically slow for MD simulations, e.g., fatigue[1–4,11] and creep[23–26] failure, may also be expedited in MMGs so that they can be simulated within reasonable MD simulation time. Concisely said, although MMGs are difficult to be produced experimentally,[14] they are ideal model systems for exploring the fundamental properties in general MGs from atomistic simulations.

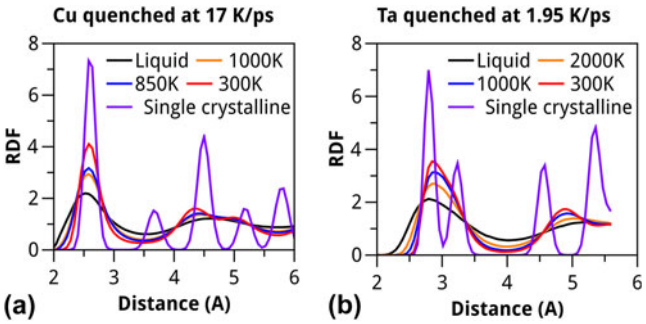


FIG. 6. The RDF of (a) Cu and (b) Ta at different temperatures during the rapid quenching.

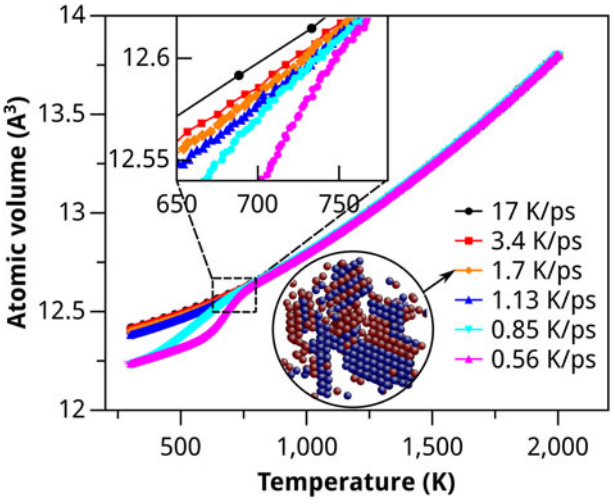


FIG. 7. The evolution of atomic volume during the rapid quenching of liquid Cu at different rates. The circular region shows the nucleated nanocrystal in the sample quenched at the rate of 1.7 K/ps. The atoms were colored according to CNA and noncrystalline atoms have been removed for clarity.

https://doi.org/10.1557/jmr.2015.130 Published online by Cambridge University Press

V. CONCLUSIONS

In summary, MMG Ta was vitrified by rapid quenching through atomistic simulations. The vitrified MMG Ta samples were found to be hardened under cyclic loading well below the yield point. It was revealed that significant structural ordering was caused during the elastic cycling without accumulating any apparent plastic strain. As the elastic cycling continued, the macroscopically undetectable structural ordering would eventually lead to the crystallization of the MMGs, which has been long conjectured in general MGs.

ACKNOWLEDGMENTS

This research was supported by Fudan University, Wuhan Institute of Physics and Mathematics, Chinese Academy of Sciences, China, and the University of Manitoba, Canada and enabled by the use of computing resources provided by WestGrid and Compute/Calcul Canada.

REFERENCES

1. C.J. Gilbert, R.O. Ritchie, and W.L. Johnson: Fracture toughness and fatigue-crack propagation in a Zr–Ti–Ni–Cu–Be bulk metallic glass. *Appl. Phys. Lett.* **71**, 476 (1997).
2. C.J. Gilbert, V. Schroeder, and R.O. Ritchie: Mechanisms for fracture and fatigue-crack propagation in a bulk metallic glass. *Metall. Mater. Trans. A* **30**, 1739 (1999).
3. M.E. Launey, R. Busch, and J.J. Kruzic: Influence of structural relaxation on the fatigue behavior of a $Zr_{41.25}Ti_{13.75}Ni_{10}Cu_{12.5}Be_{22.5}$ bulk amorphous alloy. *Scr. Mater.* **54**, 483 (2006).
4. M.E. Launey, R. Busch, and J.J. Kruzic: Effects of free volume changes and residual stresses on the fatigue and fracture behavior of a Zr–Ti–Ni–Cu–Be bulk metallic glass. *Acta Mater.* **56**, 500 (2008).
5. J.S. Langer: Shear-transformation-zone theory of deformation in metallic glasses. *Scr. Mater.* **54**, 375 (2006).
6. M. Zink, K. Samwer, W.L. Johnson, and S.G. Mayr: Plastic deformation of metallic glasses: Size of shear transformation zones from molecular dynamics simulations. *Phys. Rev. B* **73**, 172203 (2006).
7. C.A. Schuh and A.C. Lund: Atomistic basis for the plastic yield criterion of metallic glass. *Nat. Mater.* **2**, 449 (2003).
8. C. Deng and C.A. Schuh: Atomistic mechanisms of cyclic hardening in metallic glass. *Appl. Phys. Lett.* **100**, 251909 (2012).
9. C.E. Packard, L.M. Witmer, and C.A. Schuh: Hardening of a metallic glass during cyclic loading in the elastic range. *Appl. Phys. Lett.* **92**, 171911 (2008).
10. C.E. Packard, E.R. Homer, N. Al-Aqeeli, and C.A. Schuh: Cyclic hardening of metallic glasses under Hertzian contacts: Experiments and STZ dynamics simulations. *Philos. Mag.* **90**, 1373 (2010).
11. C-C. Wang, Y-W. Mao, Z-W. Shan, M. Dao, J. Li, J. Sun, E. Ma, and S. Suresh: Real-time, high-resolution study of nanocrystallization and fatigue cracking in a cyclically strained metallic glass. *Proc. Natl. Acad. Sci. U. S. A.* **110**, 19725 (2013).
12. Y.C. Lo, H.S. Chou, Y.T. Cheng, J.C. Huang, J.R. Morris, and P.K. Liaw: Structural relaxation and self-repair behavior in nanoscaled Zr–Cu metallic glass under cyclic loading: Molecular dynamics simulations. *Intermetallics* **18**, 954 (2010).
13. N. Al-Aqeeli: Strengthening behavior due to cyclic elastic loading in Pd-based metallic glass. *J. Alloys Compd.* **509**, 7216 (2011).
14. L. Zhong, J. Wang, H. Sheng, Z. Zhang, and S.X. Mao: Formation of monatomic metallic glasses through ultrafast liquid quenching. *Nature* **512**, 177 (2014).
15. S. Plimpton: Fast parallel algorithms for short-range molecular dynamics. *J. Comput. Phys.* **117**, 1 (1995).
16. R. Ravelo, T.C. Germann, O. Guerrero, Q. An, and B.L. Holian: Shock-induced plasticity in tantalum single crystals: Interatomic potentials and large-scale molecular-dynamics simulations. *Phys. Rev. B* **88**, 134101 (2013).
17. J. Li: AtomEye: An efficient atomistic configuration viewer. *Modell. Simul. Mater. Sci. Eng.* **11**, 173 (2003).
18. J. Schroers, A. Masuhr, W.L. Johnson, and R. Busch: Pronounced asymmetry in the crystallization behavior during constant heating and cooling of a bulk metallic glass-forming liquid. *Phys. Rev. B* **60**, 11855 (1999).
19. J. Schroers, W.L. Johnson, and R. Busch: Crystallization kinetics of the bulk-glass-forming $Pd_{43}Ni_{10}Cu_{27}P_{20}$ melt. *Appl. Phys. Lett.* **77**, 1158 (2000).
20. C.C. Hays, J. Schroers, W.L. Johnson, T.J. Rathz, R.W. Hyers, J.R. Rogers, and M.B. Robinson: Vitrification and determination of the crystallization time scales of the bulk-metallic-glass-forming liquid $Zr_{58.5}Nb_{2.8}Cu_{15.6}Ni_{12.8}Al_{10.3}$. *Appl. Phys. Lett.* **79**, 1605 (2001).
21. M.I. Mendelev and G.J. Ackland: Development of an interatomic potential for the simulation of phase transformations in zirconium. *Philos. Mag. Lett.* **87**, 349 (2007).
22. D. Pan, A. Inoue, T. Sakurai, and M.W. Chen: Experimental characterization of shear transformation zones for plastic flow of bulk metallic glasses. *Proc. Natl. Acad. Sci. U. S. A.* **105**, 14769 (2008).
23. B.S.S. Daniel, A. Reger-Leonhard, M. Heilmaier, J. Eckert, and L. Schultz: Thermal relaxation and high temperature creep of $Zr_{55}Cu_{30}Al_{10}Ni_5$ bulk metallic glass. *Mech. Time-Depend. Mater.* **6**, 193 (2002).
24. J.C. Gibeling and W.D. Nix: A study of the creep properties of a Ni–Fe metallic glass. *Scr. Metall.* **12**, 919 (1978).
25. F. Spaepen: Homogeneous flow of metallic glasses: A free volume perspective. *Scr. Mater.* **54**, 363 (2006).
26. C.A. Schuh and T.G. Nieh: A survey of instrumented indentation studies on metallic glasses. *J. Mater. Res.* **19**, 46 (2004).

https://doi.org/10.1557/jmr.2015.130 Published online by Cambridge University Press